

Growth of anatase titanium dioxide nanotubes via anodization

Ed Adrian Dilla*, Renato Daclan, Michael J. Defensor, Celestino Andrew M. Borja,
Arnel A. Salvador and Armando S. Somintac

Condensed Matter Physics Laboratory, National Institute of Physics
University of the Philippines, Diliman 1101, Quezon City

*Corresponding author: edilla@nip.upd.edu.ph

ABSTRACT

In this work, titanium dioxide nanotubes were grown via anodization of sputtered titanium thin films using different anodization parameters in order to formulate a method of producing long anatase titanium dioxide nanotubes intended for solar cell applications. The morphological features of the nanotubes grown via anodization were explored using a Philips XL30 Field Emission Scanning Electron Microscope. Furthermore, the grown nanotubes were also subjected to X-ray diffraction and Raman spectroscopy in order to investigate the effect of the predominant crystal orientation of the parent titanium thin film on the crystal phase of the nanotubes. After optimizing the anodization parameters, nanotubes with anatase TiO_2 crystal phase and tube length more than 2 microns was produced from parent titanium thin films with predominant Ti(010) crystal orientation and using ammonium fluoride in ethylene glycol as an electrolyte with a working voltage equal to 60V during 1-hour anodization runs.

Keywords: Nanotechnology, titanium dioxide, nanotubes, anodization

INTRODUCTION

Titanium dioxide (TiO_2) is a useful material known for its unique properties such as its high refractive index, self-cleaning effect and photocatalytic properties (Zhao et al., 2005; Jaroenworarluck et al., 2007). Titanium dioxide is often utilized as a component in biocompatible materials for bone implants (Kaneco et al., 2007; Li et al., 2009), gas sensors (Mor et al., 2006; Li et al., 2009), electronics (Kaneco et al., 2007), optical coatings (Kaneco et al., 2007) and photovoltaic cells (Mohapatra et al., 2007; Su & Zhou, 2009).

Titanium dioxide commonly exists either in rutile or anatase crystal phase. These crystal phases possess high band gaps, 3eV for rutile and 3.2eV for anatase (Zhao et al., 2005; Mor et al., 2006; Mohapatra et al., 2007). The crystal phase of titanium dioxide often affects the applications where it can be used. Anatase TiO_2 is often used in photocatalysis, dye-sensitized solar cells and photolysis while rutile TiO_2 is commonly used in industrial pigments and coatings (Mor et al., 2006).

Titanium dioxide is often fabricated as thin films or coatings. In order to fully utilize the properties of TiO_2 , it must be formed into structures that will enable it to be used efficiently for specific applications. Production of nanostructures based on TiO_2 is one of the ways to improve and utilize the properties of this material. With recent advances in materials engineering and nanotechnology, titanium dioxide nanostructures such as nanotubes, nanowires and nanorods which rectify the properties of titanium dioxide are now being used as replacements for thin films (Huang & Choi, 2007). Among these nanostructures, TiO_2 nanotubes are widely investigated due to their enhanced photocatalytic and sensing properties (Mor et al., 2006).

Titanium dioxide nanotubes are oriented nanostructures with tunable lengths and pore diameters (Paulose et al., 2006). These nanostructures are now commonly used as components in dye-sensitized solar cells and gas sensors (Li et al., 2009). TiO_2 nanotubes can be fabricated using different techniques, such as template or lithography method, hydrothermal method, sol-gel process and anodization (Kaneco et al., 2007; Li et al., 2009). Among these techniques, anodization is the most

efficient and cost effective method of fabricating self-ordered and oriented nanotubes since the completion of the whole anodization process only requires relatively cheap and accessible materials and a short duration of time unlike other techniques in fabricating of titanium dioxide nanotubes (Jaroenworarluck et al., 2007; Macak et al., 2007). Anodization is an electrochemical method of growing an oxide layer on top of a metallic layer. This method is also used to fabricate oxide nanostructures from valve metals other than Titanium, such as Aluminum, Tantalum and Niobium (Li et al., 2009). In this work, a way of producing anatase titanium dioxide nanotubes, intended for solar cell applications, with tube lengths greater than 2 microns was explored by investigating the effects of the parameters such as the crystal orientation of the parent titanium film, the type of electrolyte, anodization duration and voltage on the morphology and crystal phase of TiO_2 nanotubes.

METHODOLOGY

Glass and n-type silicon(100) were used as substrates for nanotube samples grown via anodization. The substrates were cut and subjected to a degreasing process using trichloroethylene, acetone, methanol and deionized water in order to remove unwanted grease and contaminants on the substrates.

Titanium thin film deposition was carried out after substrate preparation. Deposition was conducted for 30 minutes and 1 hour inside a chamber with a working pressure equal to 8×10^{-3} mbar and a working power equal to 150 watts to produce titanium layers with thickness approximately equal to 1 μm and 2 μm for samples anodized in hydrofluoric acid and ammonium fluoride in ethylene glycol electrolyte, respectively. In order to investigate the effects of the parent titanium thin films on the grown nanostructures, titanium thin films were deposited via RF magnetron sputtering on the substrates using two different commercial titanium sources from Chemiston Co. (source 1) and Advent Research Materials (source 2).

After deposition, the substrates deposited with a titanium film were cut into 0.5cm by 1cm samples. The samples were then mounted on the anodization setup

presented in Figure 1. The current of the system for each anodization run was monitored and recorded using a circuit connected to a computer with a Labview interface. Initial anodization runs were conducted in order to determine the metal source from which anatase titanium dioxide nanotubes will be produced. The crystal phase of the grown nanotubes was determined through Raman spectroscopy. After the initial runs, thin films from the metal source which produced anatase titanium dioxide nanotubes were subjected to anodization using different parameters. Two types of electrolytes were used during anodization, namely: hydrofluoric acid (HF) and ammonium fluoride (NH_4F) in ethylene glycol (EG). In the anodization setup, lead and silver was used as the cathode for HF and NH_4F in EG electrolyte, respectively, with the titanium thin film samples serving as the anode. Each anodization run was carried out using a constant voltage. For HF electrolytes, voltages equal to 7V, 10V, 15V and 18V were used while voltages equal to 60V, 80V, and 100V were used for NH_4F in EG electrolyte. Anodization was also conducted at different durations. For HF electrolytes, anodization was done for 3, 4, 5, and 7 minutes while anodization was conducted for 5, 15, 30 and 60 minutes for NH_4F in EG electrolyte, using a selected constant voltage. After anodization, the samples were washed with deionized water and dried with N_2 gas.

Different characterization techniques were implemented in order to investigate the effects of the

parameters on the morphology and crystallinity of the grown nanotubes. A Philips XL30 Field Emission Scanning Electron Microscope was used to observe the morphology of the nanostructures grown. The crystal structure of the parent titanium film was investigated through X-ray diffraction using a Bede D³ system. Since the as-grown nanotubes were generally amorphous, the crystal phase of the grown samples was investigated using Raman spectroscopy instead of X-ray diffraction.

RESULTS AND DISCUSSION

Crystal phase of the titanium dioxide nanotubes

Controlling the crystal phase of the grown titanium dioxide nanotubes is essential since the applications to which these nanostructures will be used are dependent on their crystal phase. In order to control the crystal phase of the grown nanotubes, the effects of the quality of the parent titanium source was investigated. The X-ray diffraction spectra of the titanium thin films are shown in Figure 2. It can be observed in Figure 2 that two crystal orientations namely, Ti(010) and Ti(002), indicated by the peaks at 35° and 38° are predominant for the titanium samples deposited using two different sources. For source 1, the intensity of the peak at 35° for Ti(010) is greater than the intensity of the peak for Ti(002) while the opposite is observed for source 2. This implies that the predominant crystal orientation of

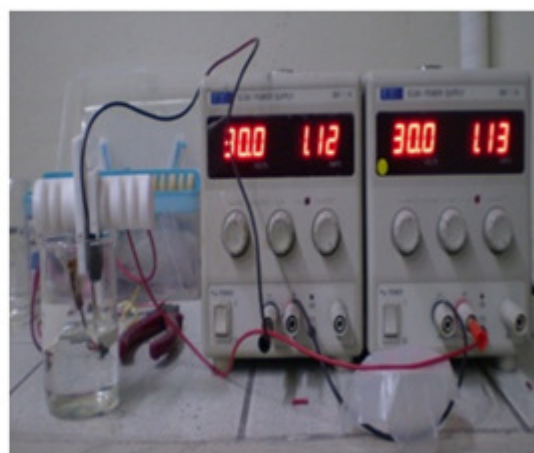
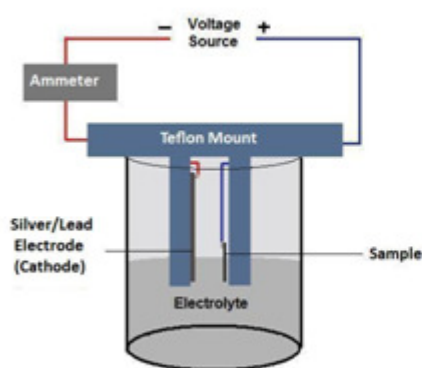


Figure 1. Setup Diagram and Actual Anodization Setup

the titanium samples from sources 1 and 2 are different from each other. Ti(010) is predominant for source 1 (Chemiston Co.) while Ti(002) is predominant for source 2 (Advent Research Materials).

Figure 3 presents the Raman spectra of the titanium dioxide nanotubes formed from the titanium samples deposited from two titanium sources. It can be observed that the nanotubes formed from different parent titanium sources exhibited different sets of peaks. For TiO₂ nanotubes grown from titanium from source 1, characteristic peaks of anatase titanium dioxide at 388, 502 and 635cm⁻¹ were observed while rutile TiO₂ peaks at 443 and 606cm⁻¹ were observed for TiO₂ nanotubes grown from the titanium from source 2.

It can be observed in Figures 2 and 3 that the crystal phase of the fabricated titanium dioxide array can be surmised from the dominant crystal orientation of the parent titanium thin film. When the intensity of the peak ascribing Ti(010) is greater than the peak for Ti(002), the resulting titanium dioxide produced during anodization is in anatase TiO₂ crystal phase. On the other hand, when Ti(002) is predominant on the parent titanium film, the nanotubes produced during anodization is in the rutile TiO₂ phase.

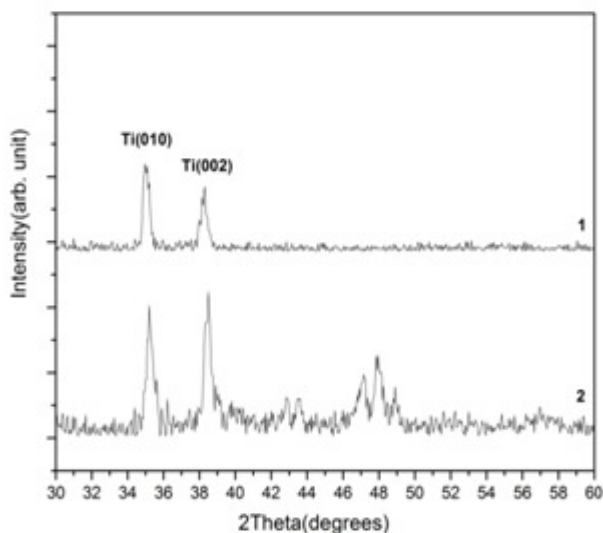


Figure 2. X-ray diffraction spectra of thin films from sources (1) and (2)

Optimization of anodization parameters

The effects of the parameters used during anodization such as voltage and anodization time are presented in this section. The discussion of these effects is divided into two subsections according to the electrolyte used during anodization, namely: A) Hydrofluoric Acid and B) Ammonium Fluoride in Ethylene Glycol electrolyte.

A. Hydrofluoric acid as an electrolyte

Titanium dioxide nanotubes are often grown via anodization using fluorine-based aqueous solutions. Among fluorine-based aqueous solutions, hydrofluoric acid (HF) is most commonly used as electrolyte in growing titanium dioxide nanotubes via anodization due to its availability and high etching rate. This section discusses the growth of titanium dioxide nanotubes via anodization in aqueous HF electrolyte.

Figure 4 shows the representative current density behaviour during anodization of samples grown using HF electrolyte. The behaviour of the current density of the system agrees with the observations made by Tang et al. (2008) and Macak et al. (2007). The periods in between each maximum or minimum in the graph, indicated by the letters a to c, correspond to the stages

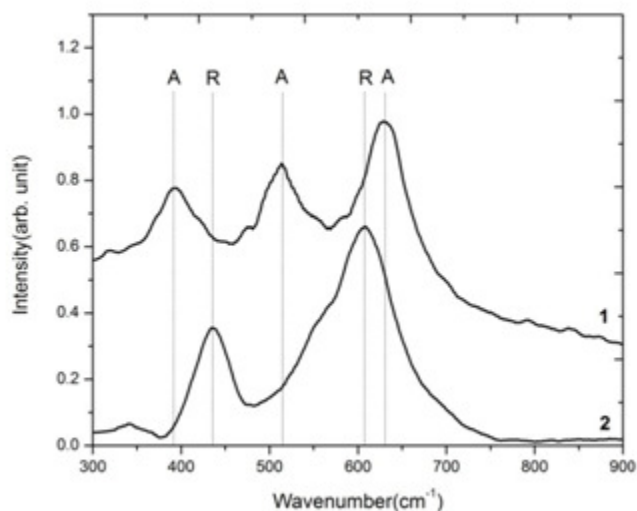
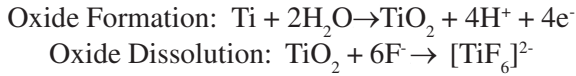


Figure 3. Raman spectra of TiO₂ nanotubes grown from the titanium thin films sputtered from sources (1) and (2). The letters A and R denote the anatase and rutile phase, respectively, of the titanium dioxide.

of nanotube growth (Macak et al., 2007). According to Macak et al., the growth of the nanotubes is mainly governed by two processes, namely: oxide formation and oxide dissolution (Macak et al., 2007). These processes are described by the chemical equations:



The sudden current drop from $t=0$ to the first minimum point at the first period, **a**, indicates the rapid formation of a barrier oxide layer on top of the titanium film layer. The drop in the current density is due to the heightened resistance of the outer layer of the titanium sample

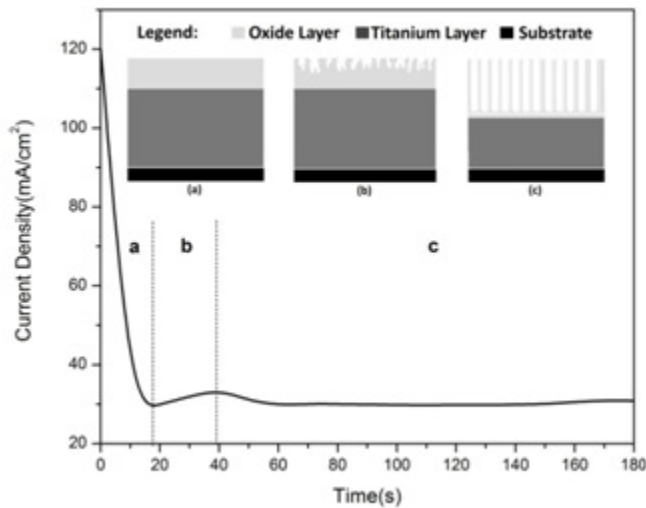


Figure 4. Current density of the anodization system during anodization

caused by the formation of the barrier oxide layer. After the period **a**, a slight increase in the current is observed which signifies the second stage of the nanotube growth. The slight increase in current density in period **b** is attributed to the localized oxide dissolution which leads to the formation of pores on selected sites in the barrier oxide layer. The third stage, period **c**, starts after the initial growth of pores on the oxide layer. A stable current density is observed in this stage as a result of the equal rate of oxide formation and dissolution. The initial pores begin to widen and grow uniformly as the current present in the system is distributed evenly among the growing pores. The pores also deepen as the fluoride ions start to dissolve the barrier oxide layer and react with the titanium ions to form the oxide nanostructures (Macak et al., 2007; Li et al., 2009).

Figure 5 presents the SEM micrograph of the samples grown at different anodization voltages. Nanotubes with different diameters, from 50nm to 130nm, were produced based on the voltage used during anodization. From the images in Figure 5, it can be observed that the diameter and length of the nanotubes increase as the anodization voltage used is increased. This agrees with the results from the work of Macak et al. (2007) and Mor et al. (2006). This increase in tube diameter and length can be attributed to effect of the distribution of the electrical current, supplied to the system, on the growing nanostructures during anodization. The variation of the tube diameter with respect to the anodization voltage used is presented in Figure 6.

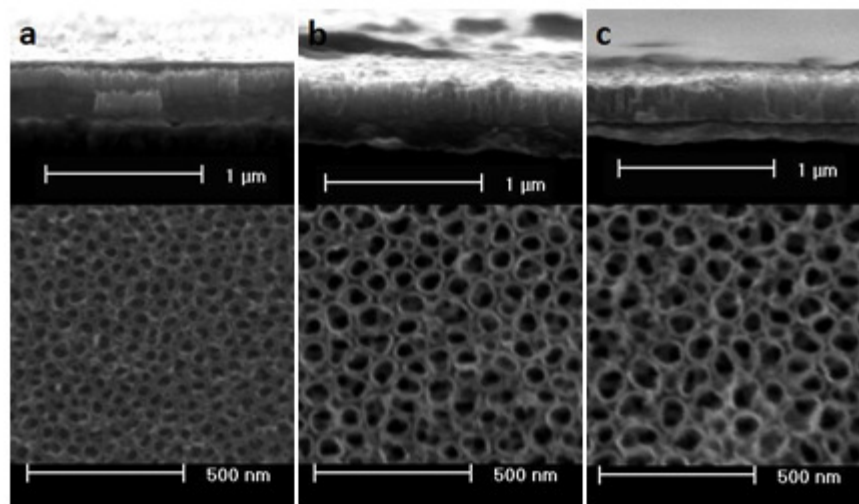


Figure 5. FE-SEM micrographs of the samples grown using a) 10V, b) 15V, and c) 18V

Figure 7 presents the SEM micrographs of the titanium dioxide nanotubes grown after different anodization durations. It can be observed that the nanotubes become more defined as the duration of anodization is increased. At $t=180$ seconds, the majority of the nanostructures are covered with a white precipitate, $\text{Ti}(\text{OH})_4$, which results from the reaction of Ti^{4+} and OH^- ions on the oxide/electrolyte interface. At longer durations of anodization, the precipitate layer recedes mainly due

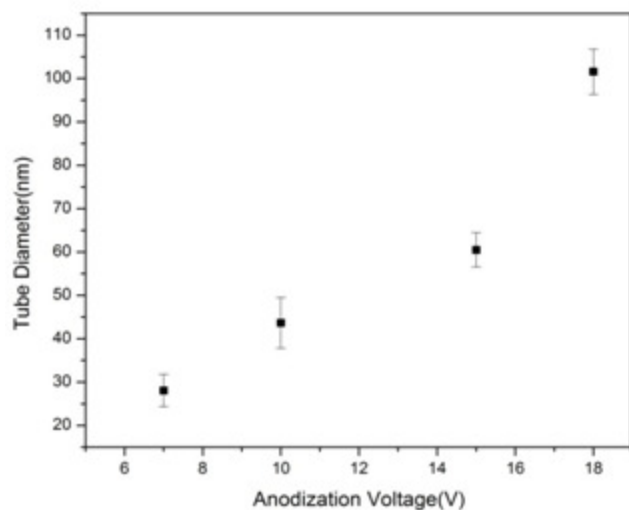


Figure 6. Variation of the nanotube diameter with the anodization voltage

to the formation $[\text{TiF}_6]^{2-}$ complex instead of $\text{Ti}(\text{OH})_4$ in the electrolyte (Macak et al., 2007). This is shown in Figure 5c, where no precipitate layer can be observed at the top of the nanotube layer. Another view of the nanotube layer, for selected anodization durations, is also presented in Figure 7. The thickness of the nanotube layer decreased from 242nm to 184nm when the duration of anodization was increased from 180 seconds to 300 seconds. The decrease in the thickness of the nanotubes may be attributed to the faster rate of oxide dissolution compared to the rate of oxide formation when the anodization time exceeds 180 seconds since the stage of uniform nanotube growth, where the rate of dissolution and oxide formation is equal, ends shortly after 180 seconds for this system as illustrated in Figure 4 (Tang et al., 2008).

Figure 8 presents the representative Raman spectra of the samples grown in HF electrolyte. Characteristic peaks of anatase titanium dioxide at 388, 502 and 635cm^{-1} are observed in the Raman spectra. This signifies that anatase titanium dioxide is predominant in the nanotubes formed during anodization.

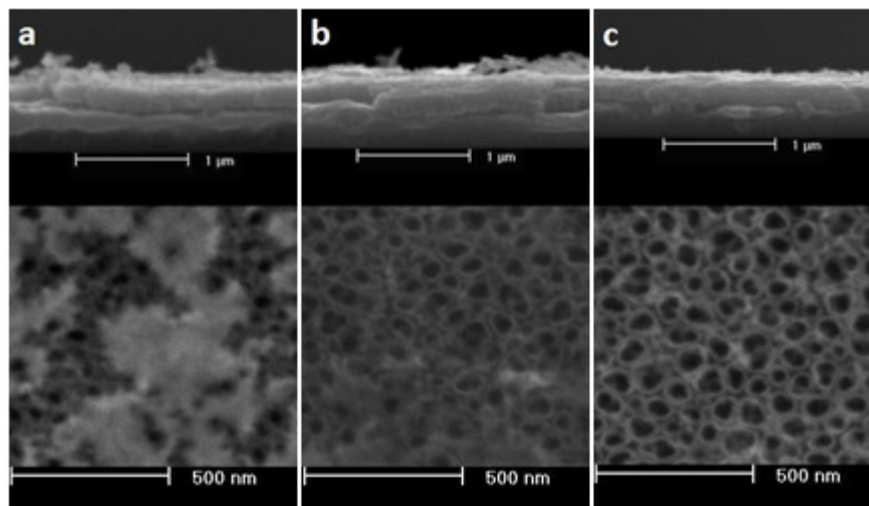


Figure 7. FE-SEM micrographs of the samples anodized for a) 180, b) 240 and c) 300 seconds. Inset shows the cross-section of the nanotube layer.

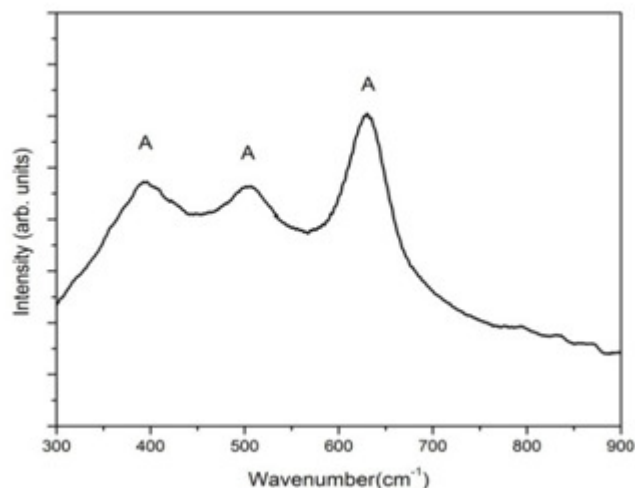


Figure 8. Raman spectra of the as-grown TiO_2 nanotube array. The symbol A denotes the anatase phase of the titanium dioxide nanotubes.

B. Ammonium fluoride in ethylene glycol as an electrolyte

The photocatalytic property of titanium dioxide nanotubes improves with the increase in the length of the nanotubes. Since the tube length of the nanotubes formed via anodization using HF electrolyte is limited, other electrolytes can be used to produce nanotubes with greater tube lengths. In this study, ammonium fluoride in ethylene glycol (EG) electrolyte was used in order to grow longer titanium dioxide nanotubes.

The behaviour of the current density during anodization in NH_4F in ethylene glycol (EG) electrolyte is shown in Figure 9. It can be observed that the current density of the system during anodization in NH_4F in EG exhibits a curve similar to the current density of the system when HF was used. It can be noted, however, that the changes in the current density of the system, which indicates the stages of nanotube formation, are set apart by longer time intervals compared to the behaviour of the current density in the case of the HF electrolyte. The mechanisms of the growth of titanium nanotubes in NH_4F in EG electrolyte and HF electrolyte are similar, although differences in the morphologies of the grown nanostructures may arise due to the differences in the chemical properties of the electrolytes. According to Prakasam et. al., the steep drop in the current density

observed in the first few seconds of anodization, period **a**, is due to the initial formation of an insulating oxide layer (Prakasam et al., 2007). Due to the insulating oxide layer, electronic conduction decreases and ionic conduction through the oxide layer increases. Electronic conduction, which is predominant mechanism at the first few seconds of anodization, is replaced by ionic conduction once the entire surface of the sample is covered by the insulating oxide layer (Prakasam et al., 2007). The stable current density following the sudden drop in current density of the system in period **b** signifies the initial formation of porous nanostructures on the oxide layer. In this stage, pores start to form on the oxide layer and continually grow until the electric field present in the system is uniformly distributed to each pore. Finally, the gradual drop of the current density followed by a region with stable current density, period **c**, signifies the formation of uniform and self-organized nanotubes which are formed as the result of the oxide formation, Ti^{4+} migration and oxide dissolution on the bottom of the initial pores (Macak et al., 2007).

The images presented in Figure 10 shows the SEM micrograph of the samples grown in NH_4F in EG electrolyte using different anodization potentials. It can be observed that the morphology of the nanostructures varies with respect to the anodization potential used. High anodization voltages lead to wider tube diameters as seen in Figures 10a-10c. It was also observed that

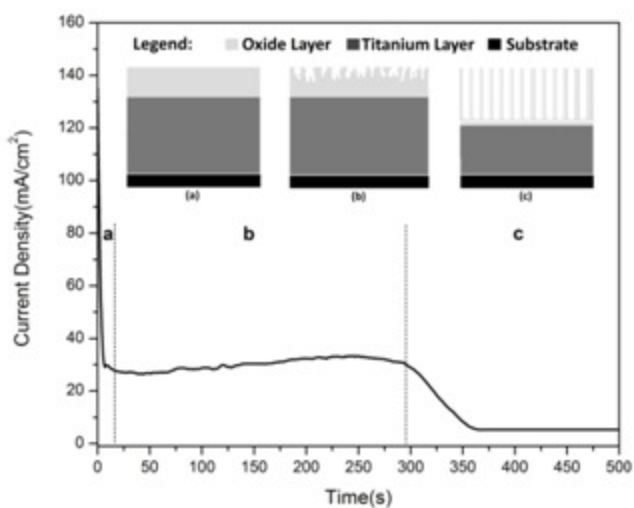


Figure 9. Current density of the anodization system during anodization

the thickness of the nanotube layer is almost the same for samples grown using 60V and 80V (2.3 microns) while a thinner nanotube layer (1.8 microns) is produced for nanotubes produced using 100V. The thinner layer produced after a 1-hour anodization run under a voltage equal to 100V is attributed to the breaking of the nanotube/oxide layer at anodization potentials greater than 60V. This is attributed to the weakening of the Ti-O bond due to polarization at high applied electric field (Tang et al., 2008). Due to the tendency of the nanotubes

produced using anodization potentials higher than 60V to breaking and peeling off from the glass substrate, the use of voltages higher than 60V may not be suitable for the production of titanium dioxide nanotubes from deposited thin films. The variation of the tube diameter with the anodization voltage is presented in Figure 11. The graph in Figure 11 exhibits a similar trend as to the case of the HF electrolyte shown in Figure 6. This result also agrees with the results of the work of Macak et al. (2007).

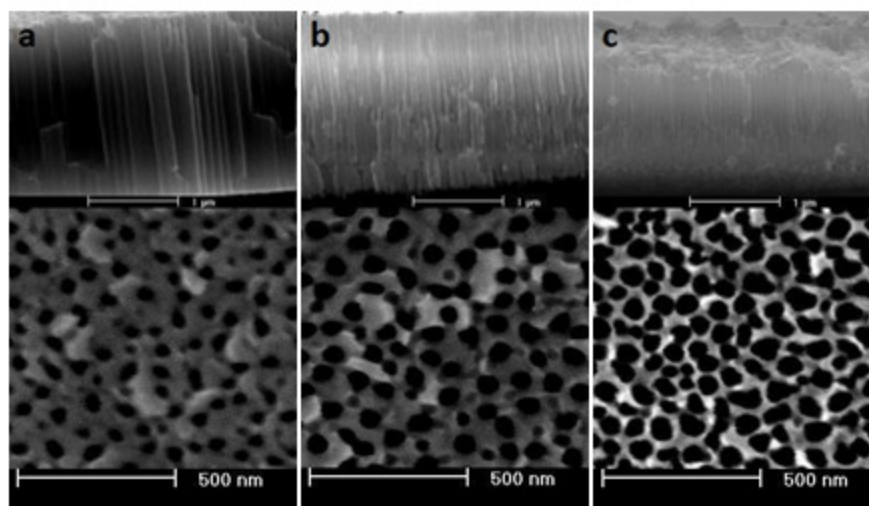


Figure 10. FE-SEM micrographs of the samples grown using a) 60V, b) 80V, and c) 100V

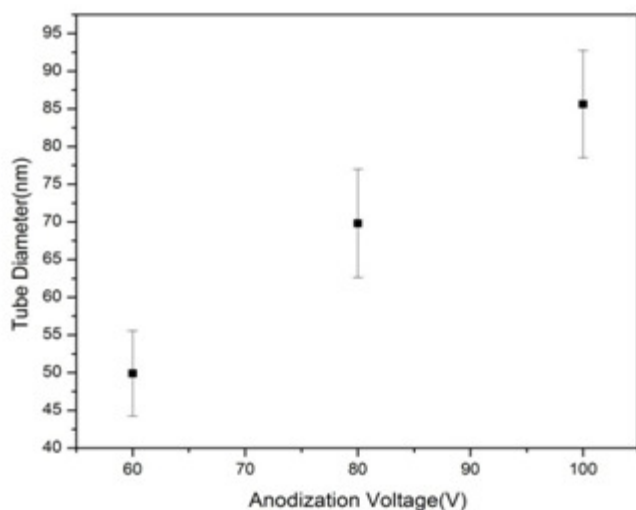


Figure 11. Variation of the nanotube diameter with the anodization voltage

Figure 12 shows the SEM micrograph of the samples grown at different durations of anodization using a constant voltage in NH_4F in EG electrolyte. Titanium dioxide nanotubes with diameters ranging from 50-80nm can be observed in the SEM images shown in Figure 12. From the presented images, it can be observed that the nanostructures are already well-developed after 5 minutes of anodization. No noticeable changes were observed in the tube diameter and the spacing of the nanotubes when the duration of anodization was increased from 5 minutes to 60 minutes. The length of the nanotubes, however, increased from 690nm to 2.3 μm when the duration of anodization was prolonged from 5 minutes to 60 minutes contrary to the result obtained in the case of the HF electrolytes. This may be due to the rapid growth rate of TiO_2

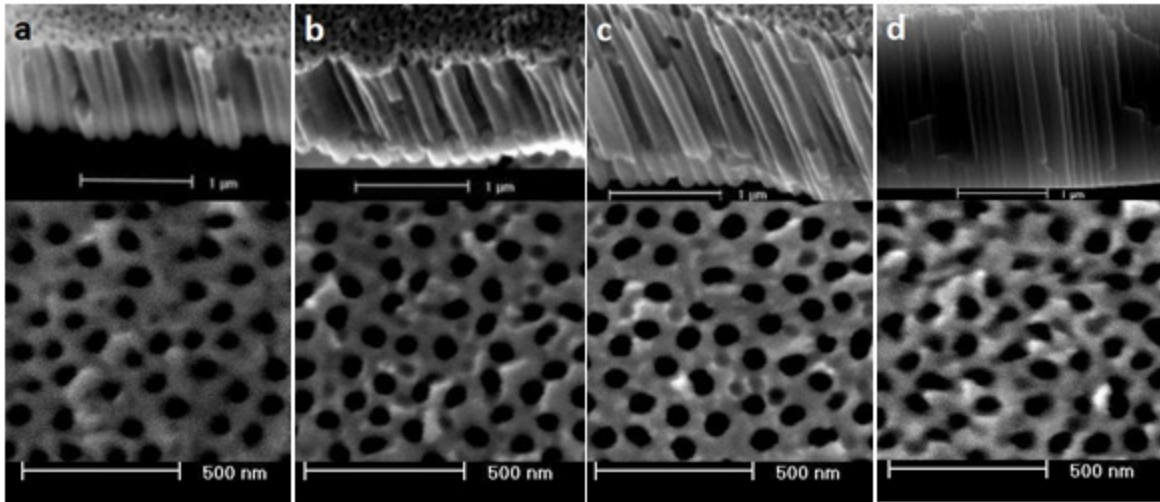


Figure 12. FE-SEM micrographs of the samples anodized for a) 5, b) 15, c) 30 and 60 minutes. Inset shows the cross-section of the nanotube layer.

nanotubes and more stable balance between oxide formation and dissolution in NH_4F in EG electrolytes compared to aqueous HF electrolytes (Prakasam et al., 2007).

The representative Raman spectra of the sample grown using NH_4F in EG electrolyte is shown in Figure 13. It can be observed that the peaks present in the Raman spectra are characteristic peaks of anatase titanium dioxide which suggests that the titanium dioxide nanotubes grown during anodization is in the anatase phase.

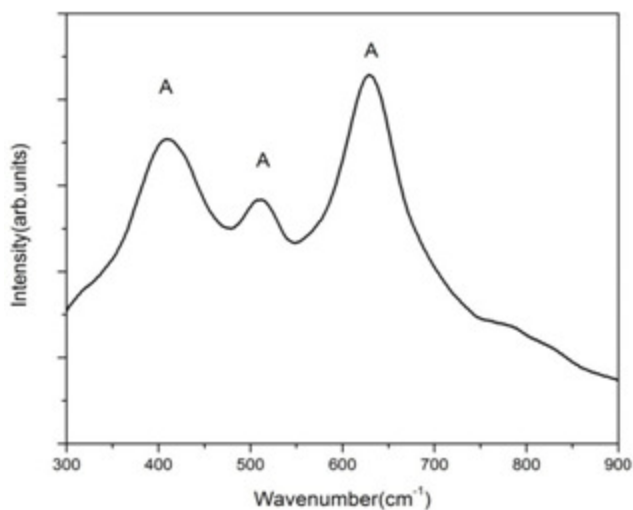


Figure 13. Raman spectra of the as-grown TiO_2 nanotube array. The symbol A denotes the anatase phase of the titanium dioxide nanotubes.

SUMMARY

Anatase titanium dioxide nanotubes, with diameters ranging from 30nm to 110nm and tube length greater than 2 microns, were successfully grown using anodization of sputtered titanium thin films. Anodization parameters, such as crystal orientation of the parent titanium thin film, anodization time, electrolyte and anodization voltage, were varied in order to explore ways of producing anatase titanium dioxide nanotubes with tube lengths exceeding 2 microns. Based on the data acquired from X-ray diffraction and Raman spectroscopy, it was observed that the crystal orientation of the parent titanium thin film dictates the crystal phase of the titanium dioxide nanotubes formed during anodization. Titanium thin films with predominant $\text{Ti}(010)$ peak result in anatase TiO_2 nanotubes while thin films with predominant $\text{Ti}(002)$ peak result in rutile TiO_2 nanotubes. From the images acquired using the FE-SEM, it was observed that the diameter of the nanotubes depend on the anodization voltage. Long nanotubes with lengths greater than 2 microns can be grown by using ammonium fluoride in ethylene glycol electrolyte instead of the common aqueous HF electrolyte and by conducting the anodization process for durations equal or more than 1 hour.

ACKNOWLEDGEMENT

This work is supported in part by grants from the University of the Philippines-Office of the Vice-Chancellor for Research and Development (UPD-OVCRD).

REFERENCES

Huang, X.-J. & Y.-K., 2007. Chemical sensors based on nanostructured materials. *Sensors and Actuators B: Chemical*, 122(2), 659-671. doi:10.1016/j.snb.2006.06.022

Jaroenworuluck, A., D. Regonini, C.R. Bowen, R. Stevens & D. Allsopp, 2007. Macro, micro and nanostructure of TiO₂ anodised films prepared in a fluorine-containing electrolyte. *Journal of Materials Science*, 42, 6729-6734. doi:10.1007/s10853-006-1474-9

Kaneco, S., Y. Chen, P. Westerhoff & J.C. Crittenden, 2007. Fabrication of uniform size titanium oxide nanotubes: Impact of current density and solution conditions. *Scripta Materialia*, 56(5), 373-376. doi:10.1016/j.scriptamat.2006.11.001

Li, Y., X. Yu & Q. Yang, 2009. Fabrication of TiO₂ nanotube thin films and their gas sensing properties. *Journal of Sensors*, 1-19. doi:10.1155/2009/402174

Macak, J. M., H. Tsuchiya, A. Ghicov, K. Yasuda, R. Hahn, S. Bauer & P. Schmuki, 2007. TiO₂ nanotubes: Self-organized electrochemical formation, properties and applications. *Materials Science*, 11, 3-18. doi:10.1016/j.cossms.2007.08.004

Mohapatra, S. K., M. Misra, V.K. Mahajan & K.S. Raja, 2007. Design of a highly efficient photoelectrolytic cell for hydrogen generation by water splitting: Application of TiO₂-x C x nanotubes as a photoanode and Pt/TiO₂ nanotubes as a cathode. *The Journal of Physical Chemistry C*, 111(24), 8677-8685. ACS Publications. Retrieved from <http://pubs.acs.org/doi/abs/10.1021/jp071906v>

Mor, G. K., O.K. Varghese, M. Paulose, K. Shankar & C.A. Grimes, 2006. A review on highly ordered, vertically oriented TiO₂ nanotube arrays: Fabrication, material properties, and solar energy applications. *Solar Energy Materials and Solar Cells*, 90(14), 2011-2075. doi:10.1016/j.solmat.2006.04.007

Mor, G., O. Varghese, M. Paulose, K. Ong & C. Grimes, 2006. Fabrication of hydrogen sensors with transparent titanium oxide nanotube-array thin films as sensing elements. *Thin Solid Films*, 496(1), 42-48. doi:10.1016/j.tsf.2005.08.190

Paulose, M., K. Shankar, S. Yoriya, H.E. Prakasam, O.K. Varghese, G.K. Mor & T.A. Latempa, 2006. Anodic growth of highly ordered TiO₂ nanotube arrays to 134 micron in length. *The Journal of Physical Chemistry, B*. doi:10.1021/jp064020k

Prakasam, H. E., K. Shankar, M. Paulose, O.K. Varghese & C.A. Grimes, 2007. A New Benchmark for TiO₂ Nanotube Array Growth by Anodization. *J. Phys. Chem*, 111(20), 7235-7241.

Su, Z., & W. Zhou, 2009. Formation, microstructures and crystallization of anodic titanium oxide tubular arrays. *Journal of Materials Chemistry*, 19(16), 2301. doi:10.1039/b820504c

Tang, Y.-xin, J. Tao, Y-yan Zhang, T. Wu, H.-junTao & Y-rong Zhu, 2008. Preparation of TiO₂ nanotube on glass by anodization of Ti films at room temperature. *Transactions of Nonferrous Metals Society of China*, 19(1), 192-198. The Nonferrous Metals Society of China. doi:10.1016/S1003-6326(08)60251-4

Zhao, J., X. Wang, R. Chen & L. Li, 2005. Fabrication of titanium oxide nanotube arrays by anodic oxidation. *Solid State Communications*, 134(10), 705-710. doi:10.1016/j.ssc.2005.02.028